

## STM spectroscopy of (MDT-TTF)<sub>2</sub>AuI<sub>2</sub>

K. Ichimura<sup>a</sup>, K. Nomura<sup>a</sup>, T. Nakamura<sup>b</sup>, T. Takahashi<sup>b</sup>, B. Hilti<sup>c</sup>, J. S. Zambounis<sup>c</sup>

<sup>a</sup>*Division of Physics, Hokkaido University, Sapporo 060-0810, Japan*

<sup>b</sup>*Department of Physics, Gakushuin University, Tokyo 171-0031 Japan*

<sup>c</sup>*Central Research Laboratories, Ciba-Geigy AG, 4000 Basel, Switzerland*

### Abstract

The electron tunneling was performed on the superconducting phase of (MDT-TTF)<sub>2</sub>AuI<sub>2</sub> using STM. The tunneling differential conductance at  $T=1.4$  K shows the superconducting energy gap structure clearly. The conductance near zero bias voltage is well reduced while the enhancement at the gap edge is observed. The obtained gap  $\Delta_0=2$  meV ( $2\Delta_0/kT_c=12$ ) is larger than that of the weak coupling limit. The shape of the spectrum, which is different from the BCS density of states, suggests the gap anisotropy. The tunneling spectrum is explained by the  $d$ -wave. The conductance well above  $T_c$  is flat. On the other hand, the pseudo gap like structure is observed near  $T_c$ .

**Keywords:** atomic force microscopy, scanning tunneling microscopy, superconducting phase transitions, organic superconductors

### 1. Introduction

It has been pointed out that the superconductivity in organic conductors, such as BEDT-TTF salts, is unconventional because of relatively higher transition temperature  $T_c$  than conventional superconductors. A lot of efforts have been made to elucidate the mechanism of the superconductivity. After that, it is recognized that the quasi-two dimensional electronic band with strong correlation plays an important role similarly to high- $T_c$  oxides.  $\kappa$ -(BEDT-TTF)<sub>2</sub>Cu(NCS)<sub>2</sub>, which has  $T_c$  of 10.4 K, is energetically investigated [1]. The evidence of the  $d$ -wave pairing was suggested by the temperature dependence of the magnetic field penetration depth, which follows the power law [2, 3].

The electron tunneling is the most useful spectroscopy in investigation of the superconducting state [4] because of its high energy resolution. Additionally, it is easy to analyze the tunneling data: the tunneling differential conductance gives the electronic density of states directly. The tunneling spectroscopy on the organic conductor was developed at first on quasi-one dimensional organic conductors. Bando *et al.* [5] reported the tunneling spectrum in the superconducting phase of (TMTSF)<sub>2</sub>ClO<sub>4</sub>. Maruyama *et al.* [6] measured the tunneling conductance for  $\kappa$ -(BEDT-TTF)<sub>2</sub>Cu(NCS)<sub>2</sub>-Al<sub>2</sub>O<sub>3</sub>-Au junctions. As the tunneling current was unstable for their junctions, one must control the tunneling barrier microscopically.

The scanning tunneling microscopy (STM) is most useful in investigating the surface electronic state because of its non-contacting tunneling configuration. There is less disturbance to the sample surface. The movable tip enables to probe the local electronic state with atomic spatial resolution. Bando *et al.* [7] measured tunneling spectra for  $\kappa$ -(BEDT-TTF)<sub>2</sub>Cu(NCS)<sub>2</sub> by STM. However, they did not discuss about the pairing symmetry. In our previous report for the tunneling at the  $b$ - $c$  surface of  $\kappa$ -(BEDT-TTF)<sub>2</sub>Cu(NCS)<sub>2</sub> [8], it was understood that the superconducting gap

is highly anisotropic. Moreover, we measured tunneling spectra at the lateral surface of  $\kappa$ -(BEDT-TTF)<sub>2</sub>Cu(NCS)<sub>2</sub> with varying the tunneling direction [9]. The in-plane gap anisotropy was directly observed and explained by the  $d_{x^2-y^2}$ -wave pairing.

An organic superconductor (MDT-TTF)<sub>2</sub>AuI<sub>2</sub>, which has  $T_c$  of about 4 K [10], is based on an asymmetric donor MDT-TTF. The arrangement of MDT-TTF molecules, which are arranged at checked pattern, is the same as that of  $\kappa$ -(BEDT-TTF)<sub>2</sub>Cu(NCS)<sub>2</sub>. The electronic band is two dimensional in  $k_x$ - $k_y$  plane. The Fermi surface of (MDT-TTF)<sub>2</sub>AuI<sub>2</sub> was reported as essentially the same as  $\kappa$ -(BEDT-TTF)<sub>2</sub>Cu(NCS)<sub>2</sub> [11]. For the symmetry of the pair wave function,  $s$ -wave symmetry was suggested by the NMR measurement [12]. Kobayashi *et al.* measured the temperature dependence of <sup>1</sup>H relaxation rate  $1/T_1$  by the field cycling method and observed an enhancement of the  $1/T_1$  just below  $T_c$ . They claimed that this enhancement corresponds to Hebel-Slichter peak expected for the isotropic gap.

Although both materials of (MDT-TTF)<sub>2</sub>AuI<sub>2</sub> and  $\kappa$ -(BEDT-TTF)<sub>2</sub>Cu(NCS)<sub>2</sub> have similar crystal and electronic band structure, the different pairing was suggested. In order to determine the symmetry of the pair wave function in (MDT-TTF)<sub>2</sub>AuI<sub>2</sub>, we investigated the superconducting state by the electron tunneling using STM, which gives the electronic density of states directly. In the present article, we report tunneling spectra obtained by STM spectroscopic measurement at the  $a$ - $b$  surface of (MDT-TTF)<sub>2</sub>AuI<sub>2</sub> and discuss about the symmetry of the pair wave function.

### 2. Experimental

Single crystals of (MDT-TTF)<sub>2</sub>AuI<sub>2</sub>, which are plate like along the  $a$ - $b$  plane, were synthesized electro-chemically. The typical dimension of the sample is about  $1 \times 1 \times 0.1$  mm<sup>3</sup>. As-grown surface of the  $a$ - $b$  plane were investigated by low temperature STM. A

mechanically sharpened Pt-Ir wire, which is attached to the tube type piezo actuator, was used as the scanning tip. The cell which contains the STM unit is filled with a low pressure of helium gas as the thermal exchange and immersed in liquid helium. In the STM spectroscopy (STS), the tunneling differential conductance was measured directly by the lock-in technique, in which 1kHz AC modulation with the amplitude of 0.05 mV was superposed in bias voltage.

### 3. Results and Discussion

In order to determine  $T_c$ , we measured the magnetic susceptibility by SQUID magnetometer. Figure 1 shows the temperature dependence of the magnetic susceptibility normalized by the Meissner susceptibility with applying the field of  $H=0.5$  G. The solid and broken lines correspond to the measurement with field cooling and zero-field cooling, respectively. The Meissner volume fraction of about 55 % indicates that the sample undergoes the bulk superconductivity.  $T_c(\text{onset})$  is determined as 4.5 K.

Figure 2 shows the temperature dependence of the tunneling differential conductance. At  $T=77$  K, the conductance is flat suggesting the metallic phase. The conductance at  $T=4.2$  K, which is close to  $T_c$ , already shows gap structure. The temperature dependence near  $T_c$  will be discussed below in detail. The conductance near zero bias voltage is reduced by about 50 % of the normal conductance. The conductance at zero bias voltage decreases with decreasing temperature. At  $T=1.4$  K, the tunneling spectrum clearly shows the energy gap structure associated with the superconducting phase. The conductance at zero bias is reduced to about 10 % of the normal conductance. The gap edge is observed clearly as the enhancement of the conductance.

We investigated the spatial variation of the tunneling conductance at a few points. Figure 3 shows the conductance with varying the tip position. Point A, B and C are aligned in the line with intervals of about 5 nm. These curves are essentially the same irrespective of the tip position. We cannot find any position dependence in the area in which the tip can be scanned by piezo actuator in our apparatus at low temperature, of about several ten nm squared.

Although noise in spectra is not a little, the reproducibility especially in low energy region is satisfactory. Figure 4 shows ten spectra which were obtained continuously at fixed position, together. The energy gap structure associated with superconducting state is well reproduced. The enhancement of the conductance appears at  $V=2$  mV, which corresponds to the edge of the superconducting gap. Another structure outside the gap edge was also found at  $V=6$  mV. However, we cannot explain well the origin of this structure. The inelastic tunneling or some kind of elementary excitation which mediates this superconductivity might bring about such a structure.

Next we are concerned with the functional form of the conductance inside the gap. At first, we examined the BCS density of states with the  $s$ -wave pairing. The solid line in Fig. 5 represents the BCS density of states with the gap  $\Delta=1.8$  meV. Then we take into account the lifetime broadening of one-electron level. We examine so called Dynes equation [13]. For many conventional superconductors, it is well known that the tunneling spectrum is well fitted by this equation. The broken line represents Dynes equation with  $\Delta=1.8$  meV and the broadening parameter  $\Gamma=0.27$  meV. As shown in the figure, remained conductance inside the gap cannot be explained by the isotropic gap. The gap anisotropy is strongly suggested.

Naively, the anisotropy is brought about by the  $d$ -wave. In the  $d$ -

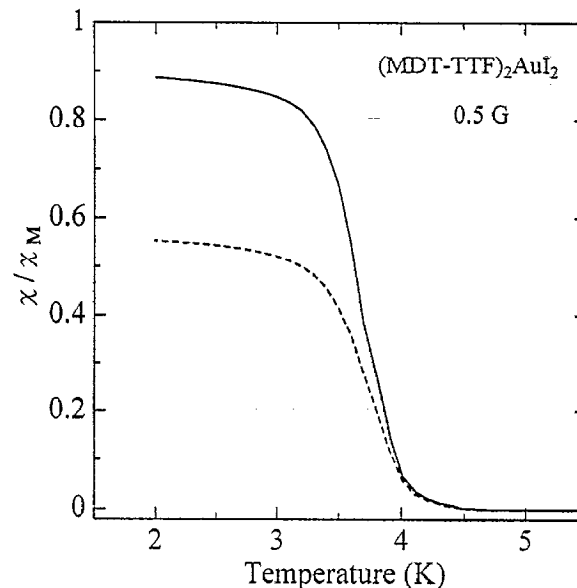


Fig. 1. Temperature dependence of the magnetic susceptibility normalized by the Meissner susceptibility. The solid and broken line correspond for the zero-field cool and field cool, respectively.

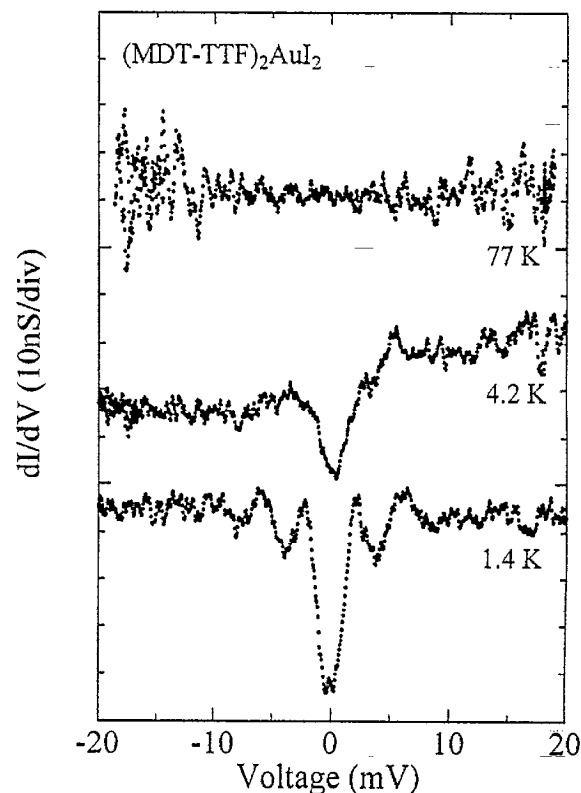


Fig. 2. Temperature dependence of the tunneling differential conductance. The zero conductance line of each curve is shifted by two divisions for clarity.

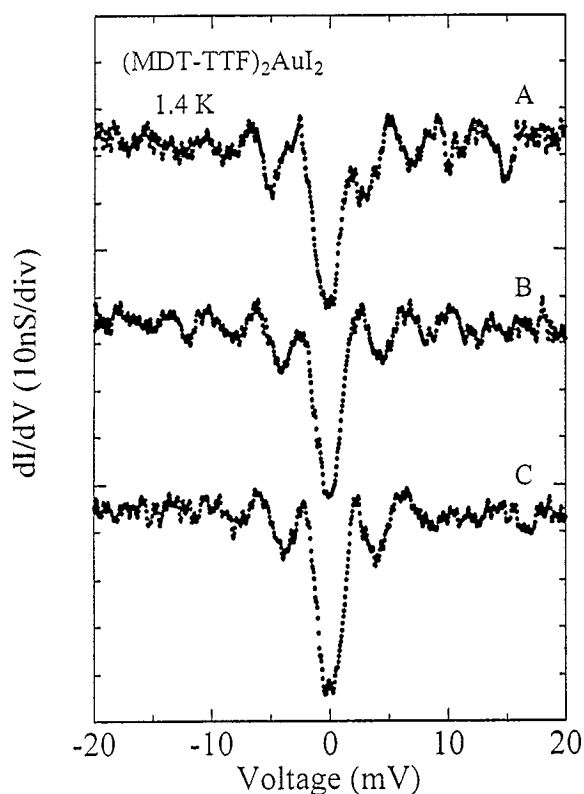


Fig. 3. Position dependence of the tunneling conductance.

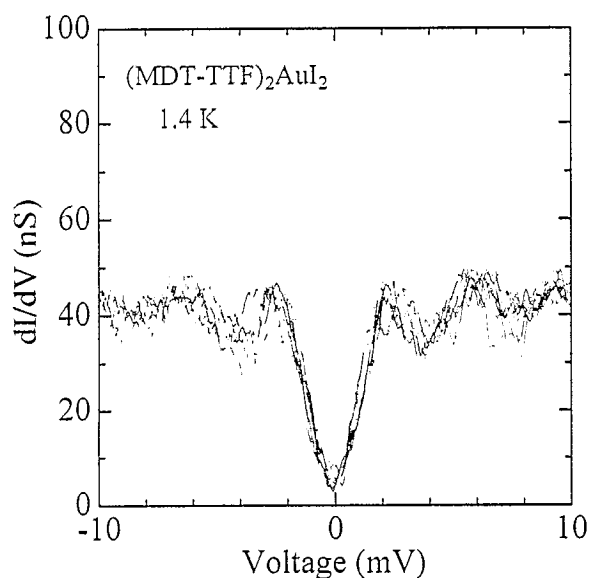


Fig. 4. Ten tunneling spectra obtained at a fixed position.

wave calculation, we adopt the  $d$ -wave as the simplest form given as,

$$\Delta(\phi) = \Delta_0 \cos(2\phi) \quad (1)$$

Figure 6 shows the fitting to the  $d$ -wave calculation. The solid line

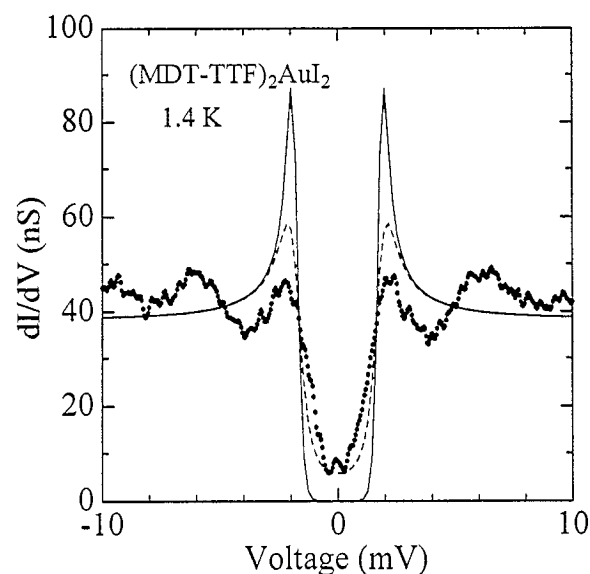
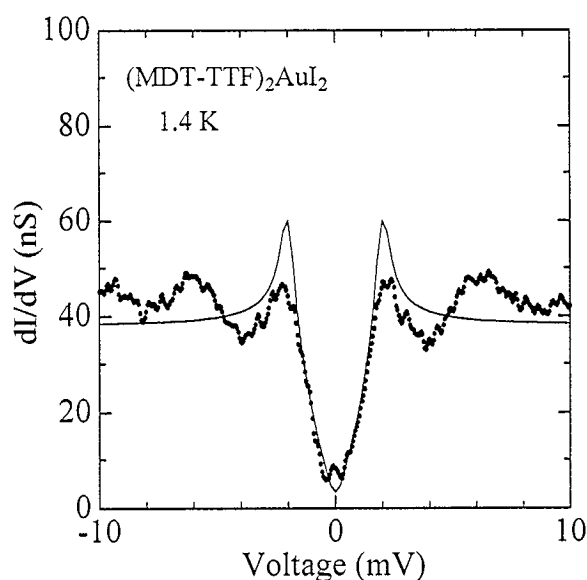


Fig. 5. Fitting to the BCS density of states.

Fig. 6. Fitting to the  $d$ -wave.

represents a calculation for the  $d$ -wave with  $\Delta_0 = 2$  meV. As shown in the figure, the calculation well reproduces the experimental result. The observed anisotropy is explained by the  $d$ -wave symmetry. The obtained gap  $\Delta_0 = 2$  meV corresponds to  $2\Delta_0/kT_c = 12$  with  $T_c = 4$  K, which is much larger than mean field value of 3.5. However, this is almost consistent with that obtained at  $\kappa$ -(BEDT-TTF)<sub>2</sub>Cu(NCS)<sub>2</sub> of 7 to 12 [8].

For the symmetry of the pair wave function, the  $d$ -wave pairing is strongly suggested. However, we cannot completely exclude the symmetry which brings about the anisotropy with the finite gap such as the anisotropic  $s$ ,  $s+d$  or  $s+id$  symmetry. But the observed large anisotropy, energy linear conductance whole inside the gap

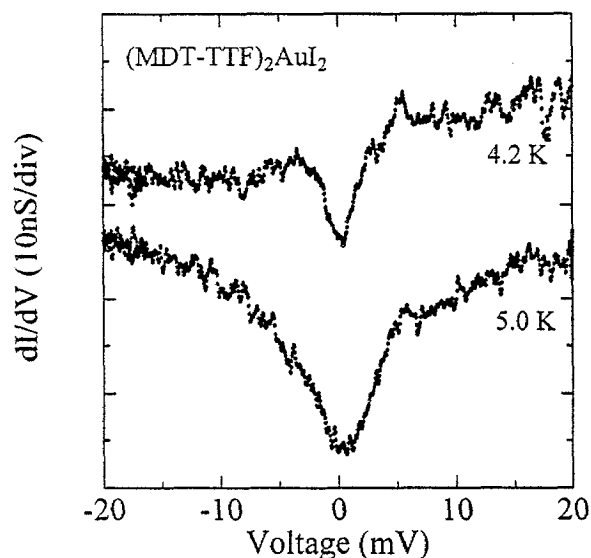


Fig. 7. Tunneling spectrum at  $T=4.2$  and 5 K. The zero conductance line for  $T=4.2$  K is shifted by two divisions for clarity.

region, is explained by the finite gap. Even if the finite gap exists, the isotropic component would be very small. From our tunneling result,  $d$ -wave is the most plausible candidate for the symmetry of the pair wave function.

On the other hand,  $s$ -wave pairing is suggested by NMR relaxation rate [12]. It is not consistent with the present tunneling result. We cannot explain completely the difference in result between the NMR and STS. One possibility is that the gap is finite but has anisotropy and that the isotropic component is relatively large. However, the STS measurement suggests that the isotropic component is very small or zero. It is an open problem.

In order to elucidate the gap anisotropy further detail, we are planning the STS at the lateral surface varying the tunneling direction like that we studied on  $\kappa$ -(BEDT-TTF)<sub>2</sub>Cu(NCS)<sub>2</sub> [9]. In this configuration, the in-plane gap anisotropy can be detected more directly.

We found that the gap structure remains even above  $T_c$ . Figure 7 shows the differential conductance at  $T=4.2$  and 5 K. At  $T=4.2$  K, relatively clear gap structure is observed. The conductance at zero bias is reduced and the gap edge is observed as a sharp peak. Indeed,  $T=4.2$  K is lower than  $T_c(\text{onset})=4.5$  K, the observed gap structure is clearer than expected. At  $T=5$  K, obviously above  $T_c$ , the broadened gap structure is observed. Therefore, we conclude that the gap exists even above  $T_c$ . This behavior is similar to pseudo gap structure recently reported in high- $T_c$  oxides. Renner *et al.* [14] reported the temperature dependence of STS spectra both on

underdoped and overdoped  $\text{Bi}_2\text{Sr}_2\text{CaCu}_2\text{O}_8$ . The energy gap associated with the superconducting state is observed below  $T_c$ . But even above  $T_c$ , the gap structure still exists. At present, we can not explain the origin and the relation between the pseudo gap and the superconducting gap.

In summary, the electron tunneling study using a low temperature STM was performed on the  $a$ - $b$  surface of single crystals of  $(\text{MDT-TTF})_2\text{AuI}_2$  in the superconducting state. The tunneling differential conductance clearly shows the energy gap structure. The tunneling spectrum is explained by the  $d$ -wave pairing with  $\Delta_0=2$  meV, correspondingly  $2\Delta_0/kT_c=12$ . The pseudo gap structure also found above  $T_c$ .

#### Acknowledgment

This work was carried out as a part of 'Research for the Future' project, JSPS-RFTF97P00105, supported by Japan Society for the Promotion of Science.

#### References

- [1] T. Ishiguro and K. Yamaji, *Organic Superconductors*, Springer-Verlag, Berlin, 1990.
- [2] K. Kanoda, K. Akiba, K. Suzuki, T. Takahashi, G. Saito, *Phys. Rev. Lett.*, **65** (1990) 1271.
- [3] L. P. Le, G. M. Luke, B. J. Sternlieb, W. D. Wu, Y. J. Uemura, *Phys. Rev. Lett.*, **68** (1992) 1923.
- [4] I. Giaever, *Phys. Rev. Lett.*, **5**, (1960) 147.
- [5] H. Bando, K. Kajimura, H. Anzai, T. Ishiguro, G. Saito, *Mol. Cryst. Liq. Cryst.*, **119** (1985) 41.
- [6] Y. Maruyama, T. Inabe, H. Urayama, H. Yamochi, G. Saito, *Solid State Commun.*, **67** (1988) 35.
- [7] H. Bando, S. Kashiwaya, H. Tokumoto, H. Anzai, N. Kinoshita, K. Kajimura, *J. Vac. Sci. Technol.*, **A8** (1990) 479.
- [8] K. Ichimura, T. Arai, K. Nomura, S. Takasaki, J. Yamada, S. Nakatsuji, H. Anzai, *Synth. Metals*, **85** (1997) 1543.
- [9] K. Ichimura, T. Arai, K. Nomura, S. Takasaki, J. Yamada, S. Nakatsuji, H. Anzai, *Physica C*, **282-287** (1997) 1895.
- [10] G. C. Papavassiliou, G. A. Mousdis, J. S. Zambounis, A. Terzis, A. Hountas, B. Hilti, C. W. Mayer, J. Pfeiffer, *Synth. Metals*, **27** (1988) B379.
- [11] A. M. Kini, M. A. Beno, D. Son, H. H. Wang, K. D. Carlson, L. C. Porter, U. Welp, B. A. Vogt, J. M. Williams, D. Jung, M. Evain, M. H. Whangbo, D. L. Overmyer, J. E. Schirber, *Solid State Commun.*, **69** (1989) 503.
- [12] Y. Kobayashi, T. Nakamura, T. Takahashi, K. Kanoda, B. Hilti, J. S. Zambounis, *Synth. Metals*, **70** (1995) 871.
- [13] R. C. Dynes, V. Narayanamurti, J. P. Garno, *Phys. Rev. Lett.*, **41** (1978) 1509.
- [14] Ch. Renner, B. Revaz, J. Y. Genoud, K. Kadowaki, Ø. Fischer, *Phys. Rev. Lett.*, **80** (1998) 149.